

A microfluidic chemical/biological sensing system based on membrane dissolution and optical absorption

This content has been downloaded from IOPscience. Please scroll down to see the full text.

2007 Meas. Sci. Technol. 18 201

(<http://iopscience.iop.org/0957-0233/18/1/025>)

View [the table of contents for this issue](#), or go to the [journal homepage](#) for more

Download details:

IP Address: 129.186.252.43

This content was downloaded on 13/02/2017 at 19:46

Please note that [terms and conditions apply](#).

You may also be interested in:

[Integration of polymer and metal microstructures using liquid-phase photopolymerization](#)

Abhishek K Agarwal, David J Beebe and Hongrui Jiang

[CVD of polymeric thin films: applications in sensors, biotechnology, microelectronics/organic electronics, microfluidics, MEMS, composites and membranes](#)

Gozde Ozaydin-Ince, Anna Maria Coclite and Karen K Gleason

[Microfluidic systems with on-line UV detection](#)

Rebecca J Jackman, Tamara M Floyd, Reza Ghodssi et al.

[A microfluidic system with integrated molecular imprinting polymer films](#)

Shih-Chiang Huang, Gwo-Bin Lee, Fan-Ching Chien et al.

[Localized and propagating surface plasmon resonance based fiber optic sensor for the detection of tetracycline using molecular imprinting](#)

Anand M Shrivastav, Satyendra K Mishra and Banshi D Gupta

[Enhanced wettability of an SU-8 photoresist through a photografting procedure](#)

Zhan Gao, David B Henthorn and Chang-Soo Kim

[Microfluidic platforms employing integrated fluorescent or luminescent chemical sensors: a review of methods, scope and applications](#)

Simon A Pfeiffer and Stefan Nagl

[A microfluidic multichannel resistive pulse sensor using frequency division multiplexing](#)

Ashish V Jagtiani, Joan Carletta and Jiang Zhe

A microfluidic chemical/biological sensing system based on membrane dissolution and optical absorption

Sudheer S Sridharamurthy, Liang Dong and Hongrui Jiang

Department of Electrical and Computer Engineering, University of Wisconsin-Madison, Madison, WI 53706, USA

E-mail: hongrui@engr.wisc.edu

Received 18 June 2006, in final form 29 September 2006

Published 30 November 2006

Online at stacks.iop.org/MST/18/201

Abstract

A microfluidic system to sense chemical and biological analytes using membranes dissolvable by the analyte is demonstrated. The scheme to detect the dissolution of the membrane is based on the difference in optical absorption of the membrane and the fluidic sample being assayed. The presence of the analyte in the sample chemically cleaves the membrane and causes the sample to flow into the membrane area. This causes a change in the optical absorption of the path between the light source and detector. A device comprising the microfluidic channels and the membrane is microfabricated using liquid-phase photopolymerization. A light emitting diode (LED) and a detector with an integrated amplifier are positioned and aligned on either side of the device. The state of the membrane is continuously monitored after introducing the sample. The temporal dissolution characteristics of the membrane are extracted in terms of the output voltage of the detector as a function of time. This is used to determine the concentration of the analyte. The absorption spectra of the membrane and fluidic sample are studied to determine the optimal wavelength that provides the maximum difference in absorbance between the membrane and the sample. In this work, the dissolution of a poly(acrylamide) hydrogel membrane in the presence of a reducing agent (dithiothreitol—DTT) is used as a model system. For this system, with 1 M DTT, complete membrane dissolution occurred after 65 min.

Keywords: chemical sensing, biological sensing, optical absorption, dissolvable membrane, microfluidics

(Some figures in this article are in colour only in the electronic version)

1. Introduction

The sensing of chemical and biological events is of critical importance in various applications [1, 2]. Currently, there are many sensing schemes, for instance surface plasmon resonance (SPR) [3–5], chemiluminescence [6–8], ellipsometry [9, 10], impedance spectroscopy [11–13], micromechanosensors [14], nanowire field-effect transistors [15, 16] and capillary zone electrophoresis with UV detection (CZE-UV) [17]. Recently, enzymatic degradation of thin

polymer films has been used for biosensing, for instance, using SPR detection [18], and impedance spectroscopy [13]. The SPR technique was capable of detecting analyte concentrations in the range of pM, but required expensive instrumentation. With impedance spectroscopy, at high electrolyte concentration (>2 mM), no changes in impedance were observed upon degradation due to similarity in the impedances of the degradable material and the surrounding electrolyte [18]. CZE-UV-based devices are relatively less portable and less cost effective and require specialized

equipment for detection, although efforts are underway to miniaturize these systems. Dissolvable hydrogels with cleavable crosslinkers have been designed and fabricated in microfluidic channels [19]. Upon exposure to certain chemicals, the crosslinks are cleaved and the hydrogels dissolve in the sample, making them promising as components of microfluidic sensors intended for one-time usage. In our previous work [20], we demonstrated a microfluidic sensing mechanism for bio/chemical analytes using membranes which dissolve in the presence of an analyte. Dissolution of the membrane causes the sample solution to flow into on-chip interdigitated electrodes, bringing about a change in the resistance between the electrodes. The approach gives an indication of the end-point of membrane dissolution, resembling the operation of an on-off switch. With 1 M analyte concentration, it took ~ 1813 s for the membrane to become porous and allow electronic detection of the analyte. However, no information regarding the concentration of the analyte can be obtained by using a single membrane.

Here, we describe a sensing system based on optical absorption which provides continuous monitoring of the state of a sensing membrane. Complete dissolution of the membrane is *not* required to estimate the presence and concentration of the analyte thereby reducing the detection time. Further, the concentration of the analyte can be determined by tracking the temporal dissolution characteristics of a *single membrane*, simplifying the system design compared to our previous work. Moreover, the time required to estimate the concentration is now shorter compared to the previous approach wherein two membranes with different dissolution times were required, the bottleneck being the membrane with longer dissolution time. A microfluidic device incorporating a bio/chemical recognition membrane is positioned in the optical path between a light emitting diode (LED) and a detector. Presence of the analyte in the sample chemically cleaves the crosslinked membrane and eventually allows the sample to flow into the membrane area. The difference between the optical absorbance of the membrane and the sample causes a change in the intensity of the light received by the detector upon dissolution. In this work, we use poly(acrylamide) (PAAm) based hydrogel membranes dissolved by dithiothreitol (DTT, the analyte). The microfabrication process is based on liquid-phase photopolymerization and is compatible with integrated circuit (IC) technology [21, 22].

2. Principle of operation

The sensing of the analyte is accomplished by the dissolution of an analyte-sensitive membrane. The event is detected by tracking the change in optical absorption of the path between a light source and a detector. The schematic diagram of the principle is shown in figure 1.

2.1. Selection of the model system

It has been shown that disulfide crosslinked PAAm hydrogels can be disintegrated in the presence of DTT [19, 20]. Here, we use this as a model for the sensing system. A disulfide crosslinked hydrogel membrane forms the sensing

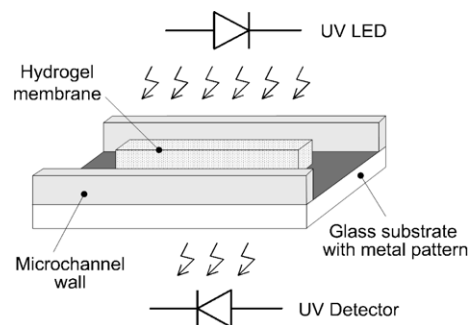


Figure 1. Principle of operation. The system detects the dissolution of a chemically sensitive homogeneously patterned membrane (here, a disulfide crosslinked poly(acrylamide)-based hydrogel) by tracking the change in optical absorption of the membrane with time. The dynamics of dissolution of the membrane (in terms of detector output voltage) is captured by a digital multimeter and recorded on a computer (not shown) for analysis.

element. The presence of the analyte (here, DTT) breaks the disulfide bonds of the hydrogel, slowly rendering it porous and ultimately dissolves it completely. The dissolution of the hydrogel is a complicated multi-step process [23]. It involves the following steps: (a) diffusion of the disulfide reducing agent into the hydrogel network, (b) reduction of the disulfide crosslinker inside the hydrogel, (c) swelling of the hydrogel during de-crosslinking as a result of decreased crosslink density, (d) disentanglement of the linear (or negligibly crosslinked) PAAm chains after de-crosslinking and, finally, (e) the dissolving of the linear PAAm into the surrounding solution. The dissolution time depends mainly on the physical dimensions of the hydrogel as well as the concentration of the analyte. Higher analyte concentrations break more bonds of the hydrogel in a given interval of time and hence show a quicker response. For example, in our sensor, a 1 M DTT solution gives a stable output in about 70 min and a 0.25 M DTT solution gives a stable output in about 125 min.

2.2. Absorption spectra of the hydrogel membrane and the sample

In order to obtain a significant change in the detector's output voltage upon dissolution of the membrane, it is necessary to employ a wavelength at which the difference between the absorption of the membrane and that of the sample is a maximum. Hence, we studied the absorption spectra of the hydrogel membrane and the sample before choosing the light source and detector. Figure 2 shows the absorption spectra of the hydrogel membrane, 1 M DTT solution and water, as measured by a spectrometer (USB 2000 Fiber Optic Spectrometer, Ocean Optics Inc., Dunedin, FL, USA). From the spectra, the absorption of both the membrane and the sample at visible wavelengths is almost equal. The difference between the absorbance increases as the wavelength moves towards the UV region (< 400 nm). It is then found that the difference between the absorbances of the membrane and DTT is maximum at ~ 340 nm. Therefore, for the experiments, an ultraviolet (UV) LED and UV photodiode with an integrated amplifier having peak emission and peak sensitivity, respectively, at 340 nm are chosen. Different

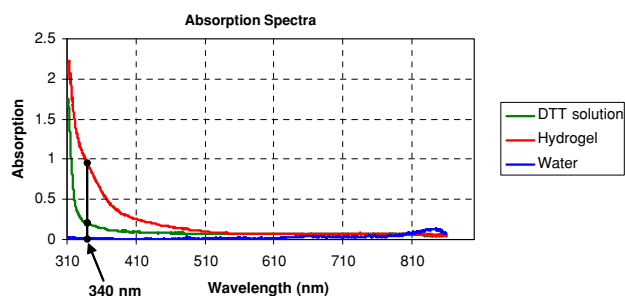


Figure 2. Choice of wavelength to be used for detection: Absorption spectra of a hydrated hydrogel membrane and the analyte (shown here as 1 M DTT solution) are compared. For better signal output upon dissolution, the difference in absorption between the hydrogel and DTT solution should be as large as possible. This difference is found to be a maximum at ~ 340 nm. Different concentrations of DTT were tested and no significant difference was observed in the absorption spectrum. Water is used as a control signal (corresponding to samples not containing the analyte).

concentrations of DTT do not cause appreciable difference in the absorption spectra. Apart from using the spectrometer, this is verified by monitoring the output voltage of the detector after introducing 1 M DTT and 0.25 M DTT sequentially into a device having no membrane. No significant change in the detector's output voltage is observed. Water is used as a control signal and hence its spectrum is also measured, representing samples that do not contain the analyte.

2.3. Operation of the sensing system

The system performs the temporal measurement of the optical absorption of the membrane in the presence of the sample. Absorption may be characterized by the Beer–Lambert law, $I_T = I_0 \exp(-\alpha L)$, where I_0 is the intensity of the incident light, I_T is the intensity of the transmitted light, α is the absorption coefficient of the absorbing material (either the membrane or the sample) and L is the absorption path length. The change in I_T is attributed to two reasons which are discussed in detail later: (i) *diffusion* of the sample solution into the membrane and (ii) *dissolution* of the membrane due to the presence of the analyte in the sample. Before diffusion/dissolution, the membrane is the absorbing material and has a relatively higher absorption (at ~ 340 nm), as compared to the sample. Upon introduction of the sample, the sample diffuses into the membrane and causes a change in the absorption of the membrane and hence, I_T . Presence of the analyte in the sample dissolves the membrane and allows the sample to flow into the region originally occupied by the membrane resulting in a further change in I_T . The difference in I_T is used to sense the dissolution of the membrane and hence the presence of the analyte. The sample is guided towards the membrane using microfluidic channels. The LED sources light onto the membrane and the detector provides an output voltage proportional to the intensity of light transmitted through the membrane. As the membrane gets dissolved, the output voltage of the detector increases. The dissolution is complete and the output voltage saturates at a particular value. By tracking the output voltage of the detector, the concentration of the analyte can be determined.

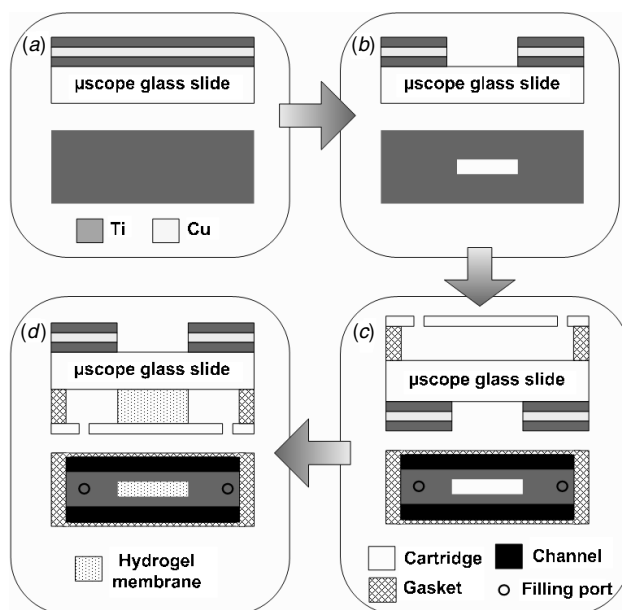


Figure 3. The fabrication process. In each panel, the cross-sectional view is represented at the top and the top view is at the bottom. The drawing is not to scale. (a) Sputtering: a microscope glass slide is coated sequentially with metal layers of Ti/Cu/Ti. These layers block light in the regions not occupied by the membrane (for detection purposes) as well as providing a mask for photopatterning the hydrogel. (b) Etching: An opening on the glass slide is created by selectively etching the metal layers. (c) Formation of the fluidic channels: the glass slide is flipped vertically and a cavity is formed by adhering a cartridge with an adhesive gasket lining to the glass slide. Liquid-phase photopolymerization is employed to form the fluidic channels. (d) Forming the hydrogel membrane: a poly(acrylamide) based pre-hydrogel liquid mixture is introduced into the fluidic channels through filling ports in the cartridge. The glass slide is again flipped vertically so that the metal layers are on top (used as a mask for photolithography) and exposed to UV. The membrane is thus self-aligned with the metal pattern.

3. Device fabrication and experimental setup

The microfluidic channels and the hydrogel membrane are microfabricated using liquid-phase photopolymerization (LP³), a process described in detail elsewhere [24]. The device is positioned between a light emitting diode (LED) and a detector. The output of the detector is monitored on a multimeter and stored on a computer.

3.1. Device fabrication

Figure 3 shows the fabrication process. A pre-cleaned microscope glass slide of dimension $7.5 \text{ cm} \times 2.5 \text{ cm} \times 1 \text{ mm}$ (Fisher Scientific, Pittsburgh, PA) is used as the substrate. First, a rectangular metal pattern is created on the substrate, which serves as a mask for photopatterning the hydrogel membrane, as well as to block light from the LED in regions not having the membrane. The substrate is sputtered sequentially with $0.05 \mu\text{m}$ titanium (Ti), $0.4 \mu\text{m}$ copper (Cu) and $0.05 \mu\text{m}$ Ti metal layers (figure 3(a)). The bottom Ti serves as an adhesion layer for Cu, while the top Ti prevents oxidation of Cu. This step is carried out in a clean room (Wisconsin Center for Applied Microelectronics, UW-Madison) with a CVC-601 dc magnetron sputterer (power: 900 W; current:

1.0 Å). A rectangular pattern of dimension $200\ \mu\text{m} \times 3\ \text{mm}$ is selectively etched into the metal layers (figure 3(b)). The top Ti is etched using hydrofluoric acid:water = 1:100. Cu is etched using acetic acid:hydrogen peroxide:water = 1:1:10. The Cu etchant does not etch the underlying Ti. The bottom Ti is etched to expose the underlying glass.

Next, the microfluidic channels are fabricated using LP³. The glass slide is flipped vertically, and a $375\ \mu\text{m}$ deep polycarbonate gasket with an adhesive liner is adhered onto the glass. The cavity thus formed between the gasket and the substrate is filled with an iso-bornyl acrylate-based pre-polymer solution. This solution consists of a monomer: isobornyl acrylate, crosslinker: tetraethylene glycol dimethacrylate, photoinitiator: 2, 2-dimethoxy-2-phenylacetophenone in the ratio (by weight) 1.9:0.1:0.06 [21, 22]. The operation of this solution resembles that of a negative photoresist. When exposed to UV radiation, the photoinitiator absorbs the light energy and uses it to bond the monomer with the crosslinker and form a polymer. The regions exposed to ultraviolet (UV) light polymerize and harden whereas the other regions remain liquid and can be flushed away with a solvent. The device is exposed to a UV light source (Acticure 4000, Exfo Life Sciences and Industrial Division, Mississauga, Ontario, Canada) through a film photomask (3600 dpi, Silverline studio, Madison, WI, USA) having the pattern of the microfluidic channels. The photopolymerization conditions are intensity = $7.8\ \text{mW cm}^{-2}$ and exposure time = 22.5 s. The liquid pre-polymer polymerizes in regions exposed to UV forming the channel walls (figure 3(c)) and the unpolymerized pre-polymer is flushed in a bath of ethanol (100%) for ~ 3 min. The device is baked on a hotplate at $50\ ^\circ\text{C}$ for ~ 30 min.

The hydrogel membrane is then defined using LP³. The fluidic channels are now filled with a poly(acrylamide)-based pre-hydrogel solution which consists of a monomer—acrylamide; crosslinker—cystaminebisacrylamide; photoinitiator—(4-benzoylbenzyl)trimethyl-ammonium chloride; co-initiator—*N*-methyl-diethanolamine; a solvent—water in the ratio (by weight) 0.15:0.00374:0.02:0.02:1 [19, 23]. The device is now flipped vertically so that the metal pattern is on top. The pre-polymer liquid does not drain from the microfluidic channels due to surface tension. It is exposed to UV light of intensity $18\ \text{mW cm}^{-2}$ for 150 s. The hydrogel membrane needs to be homogeneous. Since the pre-hydrogel liquid is homogeneous, the other factor which can cause non-homogeneity is the spatial distribution of light intensity during photopolymerization. To compensate for this, the sample is kept on a rotating circular disc during photopolymerization, which spatially averages the dose given to the sample. The hydrogel membrane is *self-aligned* with the metal pattern and any changes in the detector's output can be attributed only to changes in the membrane and not the surrounding media. The pre-hydrogel solution polymerizes to form the hydrogel membrane (figure 3(d)). The unpolymerized solution is flushed with ethanol. The device is again baked on a hotplate at $50\ ^\circ\text{C}$ for 5 min to remove the residual solvent in the hydrogel.

3.2. Experimental setup

Figure 4 shows the experimental setup. The device is coupled to a micropositioner and aligned with a UV-LED

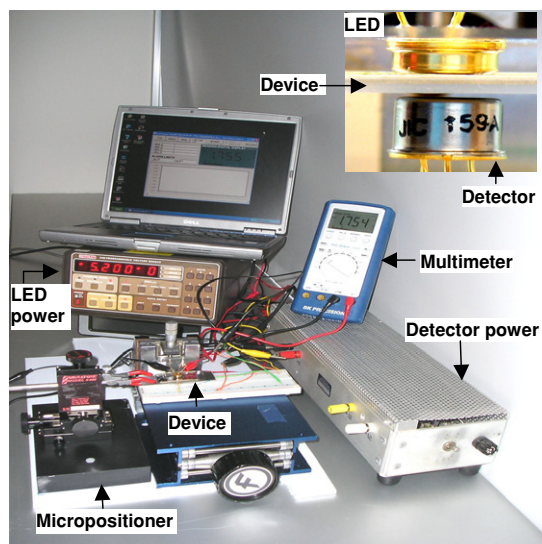


Figure 4. The experimental setup. The device is held in place using a clamp coupled to a micro-positioner. The leads of the LED are adhered onto a glass slide (coupled to a micro-positioner) having pre-drilled holes for the leads. The detector is mounted on a bread board adhered to a lab jack. Data acquisition from the detector into a computer is implemented by interfacing a multimeter which measures the output voltage of the detector and communicates with the computer through a serial interface.

light source (UVTOP-340 nm, TO-39 package, flat window, Sensor Electronic Technology, Inc., Columbia, SC, USA) and a UV photodetector with an integrated amplifier (JIC 159 A, Electro Optical Components, Inc., Santa Rosa, CA, USA). The LED is specified to have a peak emission wavelength of 340 nm and a spectrum half-width of 20 nm. Holes are drilled in a microscope glass slide and the leads of the LED are inserted into the holes and adhered onto the glass slide using double/bubble epoxy (#04004, Elementis Specialties, Inc., Belleville, NJ 07109, USA). The glass slide having the LED is coupled to a micro-positioner (Model S-926, Signatone Corporation, Gilroy, CA, USA) with the light emitting surface of the LED facing the device. The detector's sensitivity peaks at 340 nm and has a spectral range of 315 nm to 395 nm with an active area of $0.965\ \text{mm}^2$. It provides an output voltage proportional to the intensity of the UV radiation incident on its detecting surface. The detector is mounted on a bread board adhered to a lab jack (Fisher Scientific, Pittsburgh, PA, USA) and is kept fixed. An external feedback resistor of $1\ \text{M}\Omega$ is used to stabilize the gain of the amplifier in the detector. The micropositioners and the lab jack are adhered onto a board using epoxy. The UV-LED is biased at 5.2 V and the detector is powered by a 5 V dc power supply. The output of the detector is connected to a digital multimeter (Model 390 A, B&K Precision Corporation) which communicates with a computer through a serial RS-232C opto-electronic communication interface. The serial communication software provided by B&K Precision Corporation is used to store the data on the computer.

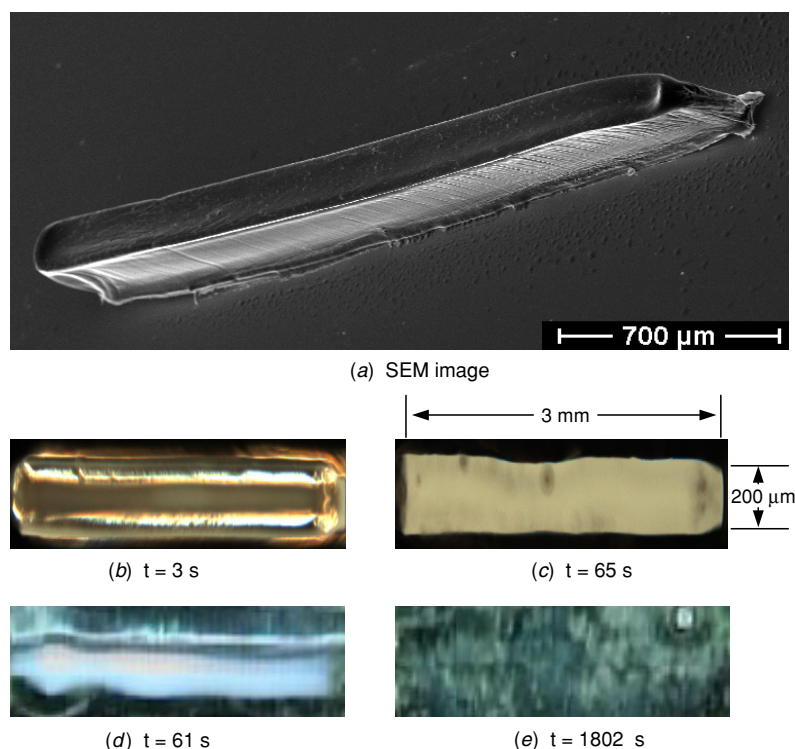


Figure 5. Diffusion and dissolution images of a $200\ \mu\text{m}$ wide hydrogel membrane in the presence of DTT. (a) Scanning electron microscope image of the poly(acrylamide) hydrogel membrane. (b) DTT has just started diffusing into the hydrogel. (c) Diffusion of DTT into the membrane makes its optical absorption close to that of the sample solution at visible wavelengths. This causes a change in the detector's output voltage which is not due to the cleavage of disulfide bonds in the hydrogel, and hence does not indicate the presence of the analyte. (d) Image of the membrane on an opaque substrate 61 s after introducing 1 M DTT. (e) After 1802 s of exposure to 1 M DTT, the membrane is partially dissolved. This causes a further change in the output voltage of the detector and indicates the presence of the analyte. Images (a) and (b) represent diffusion and are taken on a metal sputtered glass substrate with no metal in the region having the hydrogel. Images (c) and (d) represent dissolution and are taken on an opaque substrate so as to make the dissolution more visible.

4. Experiments and results

The variation in the intensity of the transmitted light (in terms of the output voltage of the detector) is recorded as a function of time for two different concentrations of DTT—0.25 M and 1 M, and water which is used as a control to show the response of the system when the sample does not contain the analyte. During experiments, the device is aligned between the LED and detector using the micropositioners coupled to the device and LED. The positioners are adjusted so that the detector shows the maximum possible output voltage when the LED is driven with 5.2 V. The sample solution is prepared by dissolving DTT (99%, SigmaAldrich) in a 0.3 M Tris buffer of pH 7.4 (Molecular biology grade, Fisher Scientific). 1 M DTT is made by dissolving 1.54 g of DTT in 10 ml of the 0.3 M Tris buffer. For other concentrations, the weight of DTT to be dissolved in the buffer is calculated proportionately. After positioning the device, the sample solution with appropriate analyte concentration is introduced into the microfluidic channel having the pattern of the hydrogel membrane through filling ports on the polycarbonate cartridge using a pipette. Upon introduction of the sample, the intensity of the transmitted light changes and is attributed to two factors: (i) *diffusion* of the sample into the hydrogel membrane soon after introducing the sample into the device and (ii) *dissolution*

of the membrane when the sample contains the analyte, as discussed below.

4.1. Diffusion of the sample/water into the hydrogel membrane

Diffusion of the sample into the membrane is one of the factors contributing to the change in the detector's output voltage. After microfabrication of the hydrogel membrane, the hydrogel is in a dehydrated state and has a relatively high absorption of the incident light as compared to the hydrated state. Figure 5(a) shows an SEM image of the hydrogel membrane. Upon introduction of the sample (or water) into the device, water diffuses into the membrane. Since water has lesser absorption than the hydrogel membrane, there is a change in the output voltage of the detector, as the optical path between the LED and the detector is then occupied partly by the sample and partly by the membrane. Figures 5(b) and (c) shows images of the membrane soon after the introduction of the sample into the system. The membrane is 3 mm long and $200\ \mu\text{m}$ wide. The curve labelled 'water' in figure 6 shows the response of the detector when the sample is water (has no DTT) and can be used as a control signal. The diffusion process does not indicate the presence of the analyte, and further information is required. This is done by testing for the dissolution of the membrane.

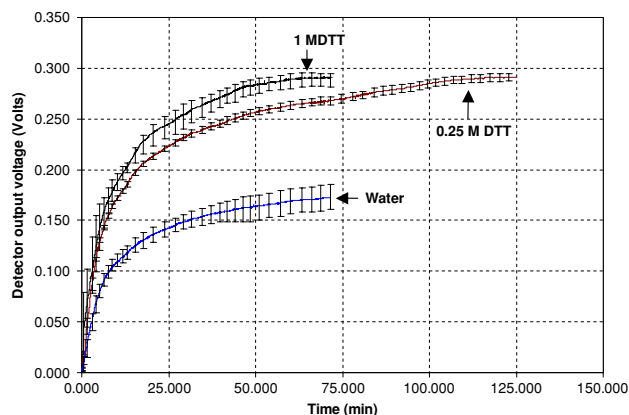


Figure 6. Response of the detector as a function of time showing the dissolution characteristics of a hydrogel membrane with two different analyte concentrations (0.25 M and 1 M) and water. Water is used as a control signal and indicates the response of the system when the sample solution does not contain the analyte. Upon introduction of the sample solution containing the analyte, membrane cleavage causes the absorption of light in the membrane area to decrease. Hence, the output voltage of the UV detector increases and saturates when the hydrogel is completely dissolved. A difference of ~ 0.3 V is observed between the polymerized and dissolved states of the membrane. By tracking the detector's output voltage with time, the concentration of the analyte can be determined, since the dissolution time of a membrane is a function of analyte concentration.

4.2. Temporal dissolution characteristics of the hydrogel membrane

After the sample diffuses into the membrane, the analyte starts dissolving the hydrogel membrane. This causes the output voltage of the detector to further increase with time and saturate upon completion of dissolution, due to a change in the optical absorption of the media between the LED and detector.

Figures 5(d) and (e) show the images of the membrane before and after dissolution. The images are taken on an opaque substrate so that the dissolution process is visible. The DTT concentration used is 1 M. In figure 5(d), the dissolution process has just started. In figure 5(e), the membrane has been dissolved. The dissolution characteristics are shown in figure 6. Following the introduction of the sample containing the analyte, as time progresses, the disulfide bonds holding the polymer hydrogel membrane are cleaved by the analyte. The sample solution flows into the membrane area and the output of the detector starts to increase, since the absorption of the sample is less than that of the membrane at the chosen wavelength (figure 2). When the membrane is completely dissolved, the output voltage of the detector ceases to increase and saturates.

Two concentrations of the analyte are studied as examples in the experiments—0.25 M and 1 M. Higher concentrations of the analyte cleave a larger number of disulfide bonds per unit time and hence results in quicker dissolution of the membrane. The final output voltage with both concentrations is the same. This shows that the hydrogel membrane is completely dissolved in both cases. A difference of ~ 0.3 V is observed between the polymerized and completely dissolved states of the hydrogel membrane. The dissolution characteristics of a membrane, thus the output voltages of the detector, depend

on the concentration of the analyte, which can be estimated by tracking the output voltage over time. For example, the dissolution characteristics for a host of analyte concentrations can be obtained and stored. By monitoring the dissolution characteristic of the analyte of unknown concentration with the stored characteristics, a best-fit estimate of the concentration can be made.

Other schemes such as impedance spectroscopy have been studied, where the membrane is patterned on interdigitated electrodes. In such a system, the effective impedance would depend not only on the membrane's impedance, but also on the analyte concentration. Hence, the impedance for different combinations of membrane thickness and analyte concentration could be the same. This makes the target concentration non-deterministic, since the composition of the sample is unknown. We found that the optical absorptions for different concentrations of the analyte were similar, making the target concentration deterministic.

5. Conclusions

A microfluidic chemical and biological sensing system using membranes dissolvable by an analyte is realized. Dissolution of the membrane by a sample solution containing the analyte causes the sample to flow into the membrane area and changes the optical absorbance of the path between a light source and a detector. The detector transduces the dissolution event into an output voltage by continuously monitoring the change in the intensity of light transmitted through the membrane. A difference of ~ 0.3 V is observed between the undissolved and dissolved states of the membrane. A single membrane can be used to estimate the concentration of the analyte by tracking the dissolution characteristics of the membrane over time. The fabrication process is compatible with conventional integrated circuit technology and the sensing system is relatively simple.

Membrane-dissolution-based sensing allows a range of species to be detected by defining membranes specific to the analyte. It may find applications in the detection of toxins which exhibit protease activity and can be highly sensitive and highly specific. For instance, neurotoxin-specific peptide sequences can be incorporated into the hydrogel network, similar to the approach reported in [25] where hydrogel scaffolds incorporate fibrinogen and polyethylene glycol. Corroborating the output voltage of the detector with the absorption spectra for different conditions such as diffusion into the membrane and its dissolution would be an interesting experiment and will be part of our future work. Presently, the sample is introduced manually into the microfluidic chamber. A sample acquisition system can be added that interfaces the sensor to the outside world and automates its operation. Such a system could leverage the one reported in [26] with integrated microfluidic components such as valves, mixers and pumps realized also using LP³. Improvements in the sensitivity of the membrane can be made by optimizing its chemical composition, physical dimensions as well as the reaction conditions. In our future work, we will extend this sensing system to other biological and chemical analytes.

Acknowledgments

This research was mainly supported by the US Department of Homeland Security (DHS) (grant number N-00014-04-1-0659), through a grant awarded to the National Center for Food Protection and Defense (NCFPD) at the University of Minnesota, and partly by the Wisconsin Alumni Research Foundation (WARF) and 3M Corporation (St Paul, MN, USA). The authors cordially thank Professor David J Beebe (University of Wisconsin-Madison) and his research group for fruitful discussions and access to their facilities. The authors also thank Professor Leon McCaughan, Megan Frisk (University of Wisconsin-Madison) and Dr Abhishek K Agarwal (Northwestern University, Evanston, IL, USA) for technical discussions and assistance.

References

- [1] Broussard L A 2001 Biological agents: weapons of warfare and bioterrorism *Mol. Diagn.* **6** 323–33
- [2] Khardori N and Kanchanapoom T 2005 Overview of biological terrorism: potential agents and preparedness *Clin. Microbiol. Newsl.* **27** 1–8
- [3] Mullett W M, Lai E P C and Yeung J M 2000 Surface plasmon resonance-based immunoassays *Methods* **22** 77–91
- [4] Homola J, Yee S S and Gauglitz G 1999 Surface plasmon resonance sensors: review *Sensors Actuators B* **54** 3–15
- [5] Sumner C, Sabot A, Turner K and Krause S 2000 A transducer based on enzyme-induced degradation of thin polymer films monitored by surface plasmon resonance *Anal. Chem.* **72** 5225–32
- [6] Dodeigne C, Thunus L and Lejeune R 2000 Chemiluminescence as diagnostic tool. A review *Talanta* **51** 415–39
- [7] Rongen H A H, Hoetelmans R M W, Bult A and Bennekom W P V 1994 Chemiluminescence and immunoassays *J. Pharma. Biomed. Anal.* **12** 433–62
- [8] Fahnrich K A, Pravda M and Guilbault G G 2001 Recent applications of electrogenerated chemiluminescence in chemical analysis *Talanta* **54** 531–59
- [9] Elwing H 1998 Protein absorption and ellipsometry in biomaterial research *Biomaterials* **19** 397–406
- [10] Striebel C, Brecht A and Gauglitz G 1994 Characterization of biomembranes by spectral ellipsometry, surface plasmon resonance and interferometry with regard to biosensor application *Biosens. Bioelectron.* **9** 139–46
- [11] Ho W H, Krause S, McNeil C J, Pritchard J A, Armstrong R D, Athey D and Rawson K 1999 Electrochemical sensor for measurement of urea and creatinine in serum based on ac impedance measurement of enzyme-catalyzed polymer transformation *Anal. Chem.* **71** 1940–6
- [12] McNeil C J, Athey D, Ball M, Ho W O, Krause S, Armstrong R D, Wright J D and Rawson K 1995 Electrochemical sensors based on impedance measurement of enzyme-catalyzed polymer dissolution-theory and applications *Anal. Chem.* **67** 3928–35
- [13] Saum A G E, Cumming R H and Rowell F J 1998 Use of substrate coated electrodes and AC impedance spectroscopy for the detection of enzyme activity *Biosens. Bioelectron.* **13** 511–8
- [14] Liu W, Montana V, Chapman E R, Mohideen U and Parpura V 2003 Botulinum toxin type B micromechanosensor *Proc. Natl Acad. Sci.* **100** 13621–5
- [15] Wang W U, Chen C, Lin K-H, Fang Y and Lieber C M 2005 Label-free detection of small-molecule-protein interactions by using nanowire nanosensors *Proc. Natl Acad. Sci.* **102** 3208–12
- [16] Cui Y, Wei Q, Park H and Lieber C M 2001 Nanowire nanosensors for highly sensitive and selective detection of biological and chemical species *Science* **293** 1289–92
- [17] Klampfl W B C W and Haddad P R 2000 Determination of organic acids in food samples by capillary zone electrophoresis *J. Chromatogr. A* **881** 357–64
- [18] Sumner C, Krause S, Sabot A, Turner K and McNeil C J 2001 Biosensor based on enzyme-catalysed degradation of thin polymer films *Biosens. Bioelectron.* **16** 709–14
- [19] Yu Q, Moore J S and Beebe D J 2002 Dissolvable and asymmetric hydrogels as components for microfluidic systems *6th Int. Conf. on Miniaturized Chemical and Biochemical Analysis Systems (Nara, Japan)*
- [20] Sridharamurthy S S, Agarwal A K, Beebe D J and Jiang H 2006 Dissolvable membranes as sensing elements for microfluidics based biological/chemical sensors *Lab on a Chip* **7** 840–2
- [21] Agarwal A K, Beebe D J and Jiang H 2006 Integration of polymer and metal microstructures using liquid-phase photopolymerization *J. Micromech. Microeng.* **16** 332–40
- [22] Agarwal A K, Sridharamurthy S S, Beebe D J and Jiang H 2005 Programmable autonomous micromixers and micropumps *J. Microelectromech. Syst.* **14** 1409–21
- [23] Yu Q 2002 Development of functional polymeric materials for microfluidic systems *PhD Dissertation* Department of Chemistry, University of Illinois, Urbana-Champaign pp 127–60
- [24] Beebe D J, Moore J S, Yu Q, Liu R H, Kraft M L, Jo B-H and Devadoss C 2000 Microfluidic tectonics: a comprehensive construction platform for microfluidic systems *Proc. Natl Acad. Sci.* **97** 13488–93
- [25] Almany L and Seliktar D 2005 Biosynthetic hydrogel scaffolds made from fibrinogen and polyethylene glycol for 3D cell cultures *Biomaterials* **26** 2467–77
- [26] Moorthy J, Mensing G A, Kim D, Mohanty S, Eddington D T, Tepp W H, Johnson E A and Beebe D J 2004 Microfluidic tectonics platform: a colorimetric, disposable botulinum toxin enzyme-linked immunosorbent assay system *Electrophoresis* **25** 1705–13